

## The segment polarity gene *armadillo* interacts with the *wingless* signaling pathway in both embryonic and adult pattern formation

MARK PEIFER, CORDELIA RAUSKOLB, MICHELLE WILLIAMS, BOB RIGGLEMAN\* and ERIC WIESCHAUS

Department of Molecular Biology, Princeton University, Princeton, New Jersey 08544-1014, USA

\*Present address: Department of Human Genetics, University of Utah School of Medicine, Salt Lake City, UT 84112, USA

### Summary

The segment polarity genes of *Drosophila* were initially defined as genes required for pattern formation within each embryonic segment. Some of these genes also function to establish the pattern of the adult cuticle. We have examined the role of the *armadillo* (*arm*) gene in this latter process. We confirmed and extended earlier findings that *arm* and the segment polarity gene *wingless* are very similar in their effects on embryonic development. We next discuss the role of *arm* in pattern formation in the imaginal discs, as determined by using a pupal lethal allele, by analyzing clones of *arm* mutant tissue in imaginal discs, and by using a transposon carrying *arm* to produce adults with a reduced level of *arm*. Together, these experiments established that *arm* is

required for the development of all imaginal discs. The requirement for *arm* varies along the dorsal–ventral and proximal–distal axes. Cells that require the highest levels of *arm* are those that express the *wingless* gene. Further, animals with reduced *arm* levels have phenotypes that resemble those of weak alleles of *wingless*. We present a description of the patterns of *arm* protein accumulation in imaginal discs. Finally, we discuss the implications of these results for the role of *arm* and *wingless* in pattern formation.

Key words: segment polarity gene, *armadillo*, *wingless*, pattern formation, *Drosophila*.

### Introduction

The segment polarity genes of *Drosophila* occupy one of the final steps in the hierarchy extending from maternal cues through gap and pair-rule genes to the final embryonic segmentation pattern (reviewed in Ingham, 1988). Embryos homozygous for segment polarity mutations develop an abnormal pattern within each segment. One can divide segment polarity mutations into classes that differ in the part of the segment affected. In mutants of the *wingless*-class, the naked cuticle of the posterior region of each segment is deleted and replaced by a mirror-image of the anterior denticle belt. This phenotype is associated with at least eight loci (*fused*, *wingless*, *gooseberry*, *hedgehog* and *cubitus interruptus*<sup>D</sup>, Nüsslein-Volhard and Wieschaus, 1980; *armadillo*, Wieschaus *et al.* 1984; *dishevelled*, Perrimon and Mahowald, 1987; *porcupine*, Perrimon *et al.* 1989).

The phenotypic similarities shared by *wingless*-class segment polarity genes suggest that these genes may function together in a biochemical pathway to send and receive positional signals in the posterior part of the segment. Based on its non-autonomy in genetic mosaics

(Morata and Lawrence, 1977) and on the fact that it encodes a secreted protein (van den Heuvel *et al.* 1989), *wingless* (*wg*) is thought to encode an intercellular signal. At least one other *wingless*-class segment polarity gene is also non-autonomous in function, and may be involved in the production or secretion of the *wg* product (*porcupine*, Klingensmith *et al.* submitted). Another gene, *armadillo* (*arm*, Gergen and Wieschaus, 1986; Wieschaus and Riggleman, 1987; Riggleman *et al.* 1990) produces cell autonomous transformations in mosaics and is expressed in all cells within the segment. Genes like *arm* may play a role in receiving and interpreting the *wg* signal, and thus enable a cell to sense its position within the segment and to choose a particular fate.

The embryonic segmental pattern persists in some form throughout development, leading to a segmented adult. The adult epidermis is formed by imaginal discs which grow and establish their final patterns during larval and pupal development. Pattern formation in imaginal discs is less well understood than that in the embryo. One obvious question is to what extent genes required for segmentation in embryos play analogous roles during subsequent patterning in discs. Embryos

homozygous for most segment polarity mutations die at the end of embryogenesis, so later requirements for their gene products cannot be assayed directly. For some loci, temperature-sensitive or weak alleles cause specific morphological abnormalities in the adult cuticle derived from the imaginal discs, arguing that these genes play a role in disc patterning (e.g. *wg*, Sharma and Chopra, 1976; *engrailed*, Kornberg, 1981). Since such weak alleles are not available for all segment polarity mutants, another approach is to create clones of mutant tissue in an otherwise wild-type animal.

We are interested in the role of one of the genes in the *wg*-class, *armadillo* (*arm*). *arm* mutants are quite similar to *wg* mutants in their effects on the embryonic pattern (Wieschaus *et al.* 1984; Klingensmith *et al.* 1989). In the embryo, *arm* acts in a cell-autonomous fashion – small clones of *arm* mutant cells are transformed in fate even when surrounded by wild-type neighbors (Gergen and Wieschaus, 1986; Wieschaus and Riggleman, 1987). The *arm* gene has been cloned and shown to encode an intracellular protein that is enriched in the region just inside the cell membrane (Riggleman *et al.* 1989, 1990). *arm* is the homolog of the mammalian protein plakoglobin, a component of desmosomes and other cell–cell junctions (Peifer and Wieschaus, 1990b). The phenotypic similarities between *arm* and *wg* in embryos suggest that the products of these genes may somehow be involved in the same signaling pathway. To see whether *arm* and *wg* also work together during later development, we examined the role of *arm* in imaginal discs. In the following paper, we describe our examination of the role of *arm* in imaginal disc development. We examined the phenotype of flies homozygous for a pupal lethal allele of *arm*, flies mosaic for *arm* and wild-type tissue, and flies in which the normal dose of *arm* product has been reduced. We have established that *arm* plays an important role in pattern formation in the discs, and have strengthened the connection between the segment polarity genes *arm* and *wg*. These results support the idea that at least these two genes are involved in a cellular pathway that is utilized during pattern formation of both the embryo and imaginal discs.

## Materials and methods

### Fly stocks and genetics

The isolation of *arm<sup>XM19</sup>*, *arm<sup>XK22</sup>*, *arm<sup>XP33</sup>*, and *arm<sup>YD35</sup>* is described in Wieschaus *et al.* (1984), the hybrid dysgenesis induced allele *arm<sup>25B</sup>* is described in Zusman *et al.* (1985) and Riggleman *et al.* (1989), and *arm<sup>H8.6</sup>* is described in Klingensmith *et al.* (1989). The severity of the embryonic phenotype of each of these mutations is compared in Peifer and Wieschaus (1990b). The *wg* mutations used are found in Nüsslein-Volhard *et al.* (1984) and Baker (1988b), while balancers and other mutants can be found in Lindsley and Grell (1968) or Lindsley and Zimm (1986). Embryos were staged as described in Wieschaus and Nüsslein-Volhard (1986). The *wg<sup>LI14</sup>* mutation is temperature-sensitive (Nüsslein-Volhard *et al.* 1984; Baker, 1988a). At 18°, embryos are wild type. At 22° embryos range from a moderate (like *arm<sup>XM19</sup>*) to a strong (like *arm<sup>YD35</sup>*) segment polarity

phenotype. Its effect on *en* expression varies in a similar fashion. The embryos in Fig. 11 and N represent embryos at the strong end of this range. To examine the expression of the *en-βgal* construct in a *wg* background, the transposon carrying this construct, which is inserted in the *en* gene (Hama *et al.* 1990), was recombined onto a chromosome carrying either *wg<sup>G22</sup>* or *wg<sup>LI14</sup>*. To identify 3rd instar larvae hemizygous for *arm<sup>H8.6</sup>*, we crossed attached-X, *C(1)RM w cv* females to *y arm<sup>H8.6</sup> f<sup>36a</sup>/y<sup>2</sup>Y67g arm<sup>+</sup>* males. Male, y progeny can then be identified both by the presence of testes and by their y cuticle structures. These larvae are hemizygous for *arm<sup>H8.6</sup>*.

### Production of genetic mosaics

In the initial experiments, young larvae (40 h ± 12 h after oviposition) were irradiated under conditions that should produce about 15 clones per 100 discs examined (Table 1). Embryos were collected on Petri dishes containing apple juice agar egg laying medium and allowed to develop to the appropriate age. After the irradiation (Gammator Model B), the embryos and apple juice agar were transferred to bottles containing standard fly food. After the adults had emerged, flies of the appropriate genotypes were collected and temporarily stored in 1:4 glycerin/ethanol. The *arm<sup>YD35</sup>* derived flies were scored for eye clones before storage. The flies were then boiled for 5 min in 10% potassium hydroxide, washed in water and mounted on slides in Faures medium. Flies were scored for the presence of bristles marked with *yellow* and *forked<sup>36a</sup>*. The positions of clones were recorded on diagrams of the different regions of the body. For the experiment involving late induction of clones, we irradiated *arm<sup>XP33</sup>/M(1)0sp* heterozygotes as mid-third instar larvae. The adults emerging from this experiment were processed as described above. The twin spot experiment involved irradiating animals heterozygous for *y arm<sup>XM19</sup>* and *singed<sup>3</sup>*, processing the flies as above, and scoring for both *yellow* and *forked*, or for *singed*. Females with homozygous *arm<sup>H8.6</sup>* germline clones were produced as described in Wieschaus and Noell (1986).

### Defects produced using an *arm* transposon

To obtain adults with reduced levels of *arm* product, we mated *arm<sup>XM19</sup>/FM7* or *arm<sup>XP33</sup>/FM7* females to males from a transformant line (BCD7) in which a P-element vector carrying 10.5 kb of *arm<sup>+</sup>* genomic sequence (Riggleman *et al.* 1989) had inserted at 36A. In contrast to most of the lines obtained with this construct, BCD7 only rescues the most hypomorphic alleles to viable adults. Males that are *arm<sup>XM19</sup>* (or *arm<sup>XP33</sup>*); *BCD7/+* die as pupae and show defects in the adult cuticle.

### Morphology, antibody staining and in situ hybridizations

Cuticles were prepared as in Wieschaus and Nüsslein-Volhard (1986), as modified by Struhl (1989). Antibody to *en/invented* was kindly provided by Nipam Patel, and antibody to β-galactosidase was purchased from Promega. All embryo fixation and antibody staining was done according to the protocol of Patel *et al.* (1989). Antibody staining of embryos was visualized using the Vecta-stain ABC kit (Vector Labs), with the addition of 0.04% nickel chloride. Imaginal discs were stained with antibodies according to the protocol of Carroll and White (1989), using the anti-N2 *arm* antibody described in Riggleman *et al.* (1990), and a rhodamine-conjugated goat anti-rabbit secondary antibody. Some preparations were also stained with an FITC conjugate of phalloidin (bodipy-phalloidin) and Hoechst 33258, as de-

scribed in Simpson and Wieschaus, 1990. Whole mount embryo *in situ* hybridizations were done according to the protocol of Tautz and Pfeifle (1989), while *in situ* hybridizations to imaginal discs was done according to the protocol of Tautz and Pfeifle (1989), as modified by Phillips *et al.* (1990).

## Results

### *arm* and *wingless* are indistinguishable in their embryonic phenotype

Klingensmith *et al.* (1989) demonstrated that the strongest mutations in *arm* and *wg* are very similar in their embryonic phenotypes. We have confirmed and extended this conclusion by using different alleles of *wg* and *arm* and by using different temperatures to produce a range in phenotypic strength. We compared in detail their effects on the embryonic pattern, on the expression of the molecular marker *engrailed* (*en*) protein, and on the survival of the cells of the posterior compartment. The effects of *arm* on *wg* expression were also examined. We evaluated *en* expression using antibody to *en/invected* protein (Patel *et al.* 1989) and survival of *en*-expressing cells using the  $\beta$ -galactosidase gene under control of the *en* regulatory region (Hama *et al.* 1990).

The different segment polarity genes are tightly interconnected. *en* is expressed in and required for the development of cells in the posterior compartment of each segment (DiNardo *et al.* 1985). While *wg* is expressed only in the most posterior cells of the anterior compartment (Baker, 1988a), both *wg* and *arm* are required for the development of a much larger region encompassing the naked cuticle of both the anterior and posterior compartments (Nüsslein-Volhard and Wieschaus, 1980; Wieschaus *et al.* 1984). *en* and *wg* are required to maintain each other's expression, and other genes of the *wg*-class are also required for the maintenance of *en* expression (DiNardo *et al.* 1988; Martinez-Arias *et al.* 1988; Klingensmith *et al.* 1989).

We found that the effects of *arm* and *wg* on the cuticular pattern and on the expression of *en* vary together over a wide range of phenotypes. In a wild-type embryo, *en* forms segmental stripes by gastrulation and *en* can still be detected at least until cuticle formation. A relatively weak mutation in either *arm* (*arm*<sup>XM19</sup>) or *wg* (weaker individuals from *wg*<sup>IL114</sup> at 22°; see Materials and methods) results in a moderate segment polarity phenotype. In these embryos, ectodermal *en* expression begins to decay during dorsal closure but significant *en* expression remains throughout embryogenesis (data not shown). A strong mutation in either *arm* (*arm*<sup>YD35</sup>) or *wg* (stronger individuals from *wg*<sup>IL114</sup> at 22°) results in a strong segment polarity phenotype. A reduction in *en* expression is detected first at late stage 9, although more dramatic effects are observed at germ-band retraction (Fig. 1E, H, and I). At even later stages of development, these embryos show an almost complete loss of ectodermal *en* expression. Finally, very strong mutants in either *arm* (embryos derived from *arm*<sup>H8.6</sup> germline clones) or *wg* (*wg*<sup>IG22</sup>) result in a very strong segment

polarity phenotype (Fig. 1A and B). In these embryos, ectodermal *en* expression is nearly absent by late stage 9 of embryogenesis (Fig. 1C and D), and no ectodermal *en* expression is observed at later stages of development (Fig. 1E, F, G). There were no significant phenotypic differences noted between *wg* and *arm*.

These experiments revealed two other features shared by *arm* and *wg*. Mutations at both loci lead to a decay in *en* expression which has similar asymmetries: the odd-numbered ectodermal *en* stripes decay before the even-numbered ones, the dorsal part of each stripe is lost first, and the maxillary segment stripe is most resistant to decay (Fig. 1E–I, M, N). These are not inherent features of the decay of *en* expression; when *en* expression decays in *extradenticle* mutant embryos, an opposite set of asymmetries is observed (Peifer and Wieschaus, 1990a). *wg* and *arm* also share another similarity in their effects on *en*. In very strong *arm* or *wg* mutant embryos, *en*-expressing cells die, as demonstrated by the disappearance of many of the cells marked by the *en*-regulated  $\beta$ -galactosidase gene (Klingensmith *et al.* 1989; Fig. 1J–L). However, in addition to this cell death, *arm* and *wg* seem to affect the presence of *en* protein more directly.  $\beta$ -galactosidase antigen persists in the ectoderm of very strong mutants of *arm* and *wg* during germ band retraction, a stage at which ectodermal *en* antigen is clearly no longer detectable (Compare Fig. 1J–L with E–G). Therefore, the absence of *en*-expressing cells appears to be due, at least initially, to a failure to maintain *en* expression rather than merely to cell death. DiNardo *et al.* (1988) came to a similar conclusion with respect to the effect of *wg* on *en*. Together, our results suggest that *arm*, like *wg*, is required to maintain *en* expression.

We also examined the expression of *wg* RNA in embryos with strong or very strong *arm* phenotypes. In the very strong mutant embryos, *wg* RNA is no longer detectable by late stage 9 (Fig. 1O and P). Interestingly, a pair-rule pattern of loss of *wg* expression is observed for the strong *arm* mutant, with expression again lost dorsally before ventrally (Fig. 1Q). This loss may reflect either loss of *wg* expression or death of the *wg*-expressing cells. The timing and pattern of loss of both *en* and *wg* expression in *arm* mutants are very similar, if not identical.

### *The requirement for wingless in the imaginal discs*

The similarity of *arm* and *wg* in embryos led us to compare their effects in imaginal discs. We will quickly review *wg* action and expression in imaginal discs. *wg* is required during larval stages for the development of most or all imaginal discs (Baker, 1988a, 1988b). Weak *wg* mutants survive to adulthood, although they often fail to emerge from their pupal cases. These adults have defects in many imaginal disc derivatives (Sharma and Chopra, 1976; Baker, 1988b). Small clones of *wg* cells can be rescued by wild-type neighbors, thus *wg* acts non-autonomously (Morata and Lawrence, 1977). In weak *wg* mutants, a variety of defects are found (Sharma and Chopra, 1976; Baker, 1988b; Fig. 2E–H, Fig. 4; the phenotypes are described in more detail in

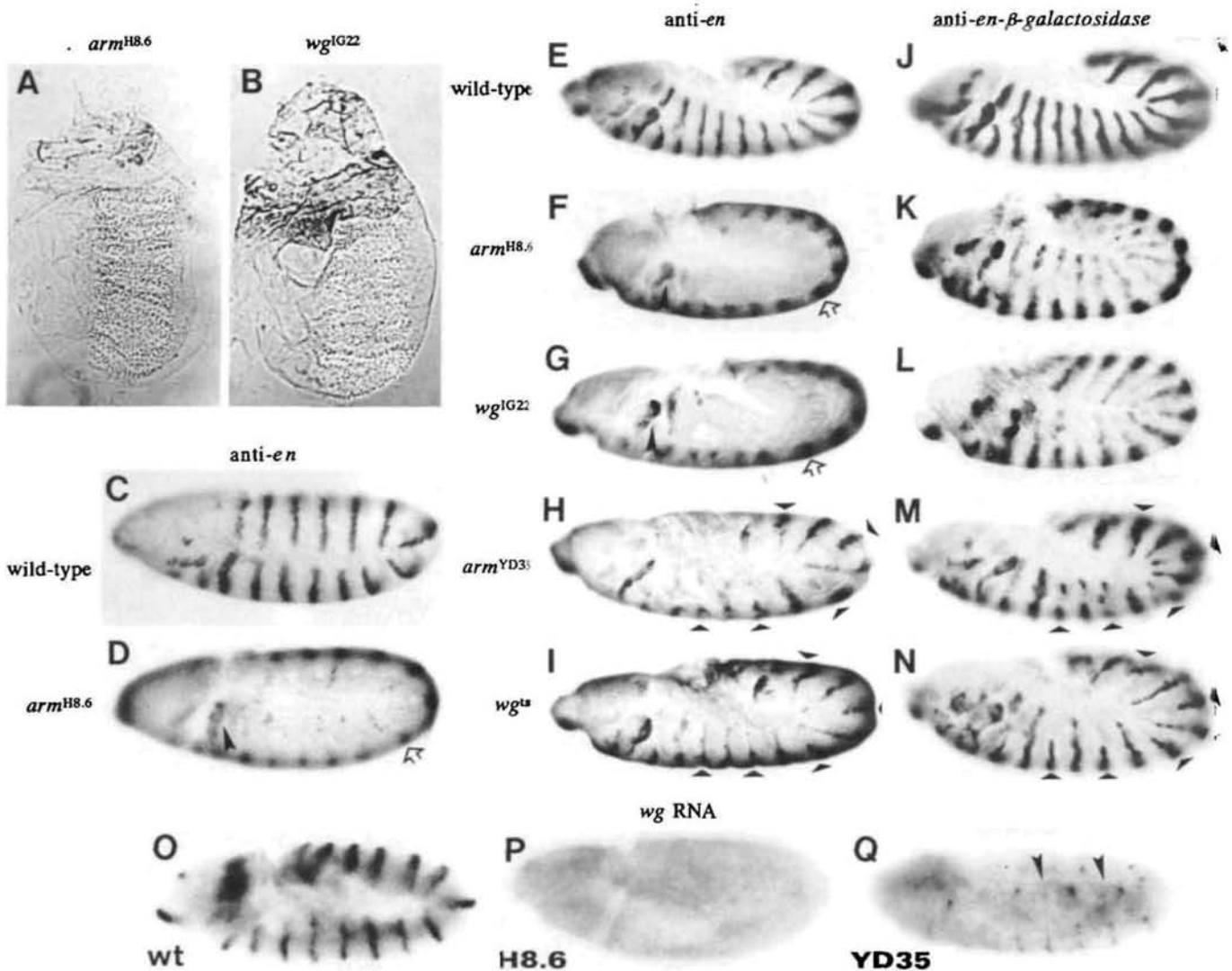


**Fig. 1.** *arm* and *wg* are indistinguishable in their embryonic phenotypes. A and B show ventral views with anterior to the top, while in C–Q all embryos are oriented with anterior to the left and dorsal up. (A, B) Cuticle preparations demonstrating the strongest phenotype of *arm* and *wg*. Maternal *arm* product is contributed to the embryo during oogenesis (Wieschaus and Noell, 1986). To remove maternally supplied *arm* and to obtain the strongest mutant phenotype, we generated germ line clones (GLC) using the temperature-sensitive *arm*<sup>H8.6</sup> allele at 25° (Klingensmith *et al.* 1989). *wg*<sup>IG22</sup> is probably a null. (C and D) *en* expression in late stage 9 wild-type (C) and *arm*<sup>H8.6</sup> GLC-derived embryos (at 25°; D). A substantial loss of *en* expression is observed in the ectoderm of the mutant embryos, while maxillary segment (arrowhead) and nervous system (open arrow) staining remain unaffected. (E–G) *en* expression in germ band retracting (stage 12) wild-type embryos (E), and in very strong mutants, *arm*<sup>H8.6</sup> GLC at 25° (F) and *wg*<sup>IG22</sup> (G). In both mutants, complete loss of ectodermal *en* expression is observed. (H and I) *en* expression in the mutants, *arm*<sup>YD35</sup> (H) and *wg*<sup>IL114ts</sup> at 22° (I). The odd-numbered *en* stripes are lost first (indicated by an arrowhead) and *en* expression is lost laterally before ventrally. This pattern is transient; *en* expression decays rapidly in all segments. (J–L) *engrailed*- $\beta$ -galactosidase (*en*- $\beta$ -gal) expression at stage 12 in wild-type (J), *arm*<sup>H8.6</sup> GLC at 25° (K), and *wg*<sup>IG22</sup> embryos (L). Note that  $\beta$ -gal antigen is still detectable in the very strong mutants. (M, N). *en*- $\beta$ -gal expression in stage 12 mutants *arm*<sup>YD35</sup> (M) and *wg*<sup>IL114ts</sup> at 22° (N). The pair-rule pattern seen here is transient. (O–Q). *wg* RNA expression in wild-type (O) and *arm* mutant embryos (P and Q). A complete loss of *wg* expression is observed by late stage 9 in *arm*<sup>H8.6</sup> GLC embryos at 25° (P) as compared to wild-type (O). In the mutant *arm*<sup>YD35</sup> (Q), *wg* expression is lost in a pair-rule pattern. In addition, the lateral patches of *wg* expression disappear (arrowheads) before the ventral stripes.

the legend to Fig. 2). Wing and haltere are transformed into notum and metanotum. Legs show proximal duplication and distal branching, resulting from the loss of ventral structures and their replacement by duplicated dorsal structures. In the head, specific structures are lost, with the antennae and the head capsule most

sensitive and the post-orbital region and adjacent eye facets least sensitive. Defects are also seen in the proboscis and abdomen (Baker, 1988a). Molecular analysis has provided possible explanations for some of these observations. *wg* encodes a secreted protein that may act as a signal between cells (Baker, 1987;

Rijsewijk *et al.* 1987; Cabrera *et al.* 1988; van den Heuvel *et al.* 1989); this may explain why wild-type cells can rescue mutant neighbors. In embryos (Baker, 1987, 1988a) and imaginal discs (Baker, 1988b), *wg* RNA is produced in only a subset of the cells which require it, again suggestive of a cell-cell signaling role.

Patterns of *wg* expression vary between different imaginal discs (e.g. Fig. 2A–D). Related patterns are seen in the leg and antennal discs, which share prominent expression in the ventral quadrant of the disc (Fig. 2B and 2D). Wing (Fig. 2A) and haltere discs share a different pattern of expression more complex than that of the legs. Genital discs show medial *wg* expression (Fig. 2C). In most cases, structures that are most frequently deleted in *wg* mutants are located in regions that express high levels of *wg* transcript (Baker, 1988b; Fig. 2).

#### armadillo activity is required during the development of the imaginal discs

While most alleles of *arm* are embryonic lethals, *arm<sup>H8.6</sup>* is a pupal lethal at 18°C (Klingensmith *et al.* 1989). We have characterized the terminal phenotype of these mutant animals by using larval markers to identify homozygous mutants. No adult cuticle is found in dissected dead pupae. Mutant late third instar larvae have extremely small imaginal discs (Fig. 3A vs. B), suggesting that *arm* is required for disc development.

To strengthen this conclusion, we adopted a complementary approach. While animals homozygous for *arm* die, one can produce and examine small patches of homozygous *arm* tissue in an otherwise wild-type adult. We used gamma-rays to induce mitotic recombination in *y arm<sup>f<sup>6a</sup></sup>/Minute(1)0sp* first-instar larvae. Half of

the progeny cells of a mitotic recombination event become homozygous for the *Minute* and die, and half become homozygous for *arm*. *arm* clones are marked with the cuticular markers *yellow* and *forked*, allowing homozygous mutant cells to be distinguished from their *arm<sup>+</sup>* neighbors. Homozygous *arm* clones have a growth advantage over their *Minute/arm* neighbors. We examined the survival and phenotype of *arm* clones in adults, using similarly induced clones of marked *arm<sup>+</sup>* cells as a control.

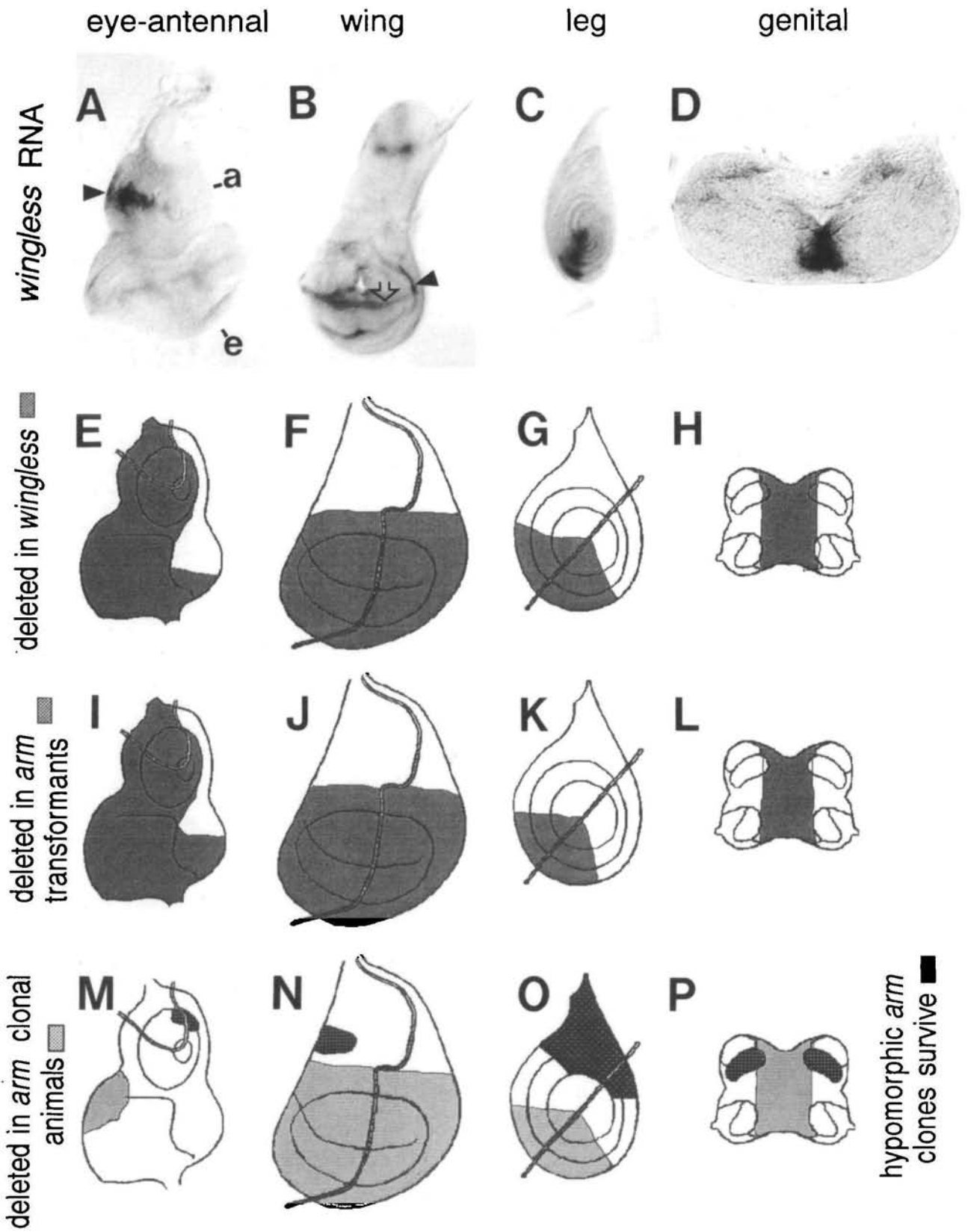
Because of their *Minute<sup>+</sup>* growth advantage, the *arm<sup>+</sup>* control clones were usually quite large, comprising up to 50% of the surface derivatives of a given disc. Clones of this size homozygous for strong *arm* alleles (*arm<sup>YD35</sup>*, *arm<sup>XK22</sup>*, or *arm<sup>XP33</sup>*; Table 1) were never found in any imaginal disc. Some small patches of one to three marked bristles were detected, but at only 3–5% of the overall frequency of control clones. Large clones homozygous for strong *arm* alleles apparently die. To determine whether clones induced later in larval development survive better, we irradiated *arm<sup>XP33</sup>/M(1)0sp* heterozygotes as mid-third instar larvae. By this stage, control *arm<sup>+</sup>* clones were relatively small, due to the limited time for growth between irradiation and metamorphosis (e.g. in the eye-antennal disc, the average size was 2.0 (s.d.1.9) bristles). When *arm* heterozygotes were irradiated at this late larval stage, more homozygous *arm* clones were detected than following earlier irradiations, but the recovery rate remained substantially lower than that of *arm<sup>+</sup>* controls and the mutant clones were significantly smaller (Table 2). This suggests that *arm<sup>+</sup>* activity is still required in late larval and pupal stages. Moreover, the survival of late clones might simply be attributed to the fact that, given the late stage of the irradiation,

Table 1. *arm* clones in imaginal discs

| Genotype  | Head      | Labial     | Humerus   | Wing      | Leg       | Tergite   | Sternite  | Genitalia | Analia    |
|---|-----------|------------|-----------|-----------|-----------|-----------|-----------|-----------|-----------|
| (a) Control clones  |           |            |           |           |           |           |           |           |           |
| Exp. A  |           |            |           |           |           |           |           |           |           |
| <i>y</i>  | 155/244*  | 17/100     | 26/197    | 56/197    | 115/197   | 68/30     | 53/30     | 13/101    | 15/101    |
| Exp. B  |           |            |           |           |           |           |           |           |           |
| <i>ywf</i>  | 38/129    | 4/129      | 6/129     | 9/129     | 49/129    | 47/60     | 10/60     | 6/129     | 3/129     |
| Exp. C  |           |            |           |           |           |           |           |           |           |
| <i>ywf</i>  | 61/130    | 5/130      | 13/95     | 15/95     | 45/55     | 40/15     | 10/15     | 8/140     | 6/140     |
| (b) <i>arm</i> mutant clones, arranged from strong to weak based on embryonic phenotype |           |            |           |           |           |           |           |           |           |
| <i>YD35</i>   | 0/129     | 0/129      | 0/76      | 0/76      | 0/76      | 0/20      | 0/20      | 0/76      | 0/76      |
| (Exp. C)  | <b>0</b>  | <b>0</b>   | <b>0</b>  | <b>0</b>  | <b>0</b>  | <b>0</b>  | <b>0</b>  | <b>0</b>  | <b>0</b>  |
| <i>XK22</i>   | 0/102     | 3/254      | 0/177     | 1/177     | 1/59      | 0/40      | 0/40      | 1/254     | 1/254     |
| (Exp. A)  | <b>0</b>  | <b>7</b>   | <b>0</b>  | <b>2</b>  | <b>3</b>  | <b>0</b>  | <b>0</b>  | <b>3</b>  | <b>3</b>  |
| <i>XP33</i>   | 1/98      | 6/202      | 0/141     | 1/141     | 0/61      | 0/30      | 0/30      | 0/130     | 0/130     |
| (Exp. A)  | <b>2</b>  | <b>17</b>  | <b>0</b>  | <b>2</b>  | <b>0</b>  | <b>0</b>  | <b>0</b>  | <b>0</b>  | <b>0</b>  |
| <i>XM19</i>   | 3/121     | 17/100     | 18/254    | 24/254    | 95/254    | 3/62      | 0/62      | 0/175     | 10/175    |
| (Exp. A)  | <b>4</b>  | <b>100</b> | <b>55</b> | <b>33</b> | <b>64</b> | <b>2</b>  | <b>0</b>  | <b>0</b>  | <b>38</b> |
| <i>25B</i>  | 9/200     | 6/200      | 7/200     | 6/200     | 27/200    | 6/96      | 1/96      | 0/200     | 1/200     |
| (Exp. B)  | <b>15</b> | <b>97</b>  | <b>75</b> | <b>43</b> | <b>36</b> | <b>8</b>  | <b>6</b>  | <b>0</b>  | <b>22</b> |
| <i>H8.6</i>   | 32/169    | 9/169      | 2/120     | 3/120     | 41/80     | 17/20     | 6/20      | 1/160     | 2/160     |
| (Exp. C)  | <b>40</b> | <b>138</b> | <b>12</b> | <b>16</b> | <b>63</b> | <b>11</b> | <b>15</b> | <b>2</b>  | <b>44</b> |

\* Number of clones recovered in particular discs/Number of irradiated heterozygous individuals examined. % recovery of *arm* clones compared to the control are given in bold type.

The number of irradiated individuals examined for each disc type varied and was chosen based on the control frequency. The identity of the appropriate control is indicated for each mutant.



subsequent growth was insufficient to dilute the *arm*<sup>+</sup> product derived from the heterozygous mother cell. The failure to obtain clones of strong alleles indicates

that *arm*<sup>+</sup> activity is required in all imaginal discs, but does not necessarily imply that all regions of those discs require equal amounts of *arm* product. In embryos,



**Fig. 2.** *wg* and *arm* in imaginal discs. (A–D) *wg* RNA expression. These patterns were described by Baker (1988b). Imaginal discs were hybridized with probe to a *wg* cDNA. (A) *wg* expression in the eye–antennal disc. We have not analyzed the expression pattern in the eye disc (labeled ‘e’). The pattern in the antennal disc (labeled ‘a’) resembles that in the leg discs, with expression in a ventral wedge (arrowhead). (B) *wg* expression in the wing imaginal disc. Expression in this disc is complex, and includes a stripe across the wing pouch (arrow – out of focus in this view; see Fig. 5I), a ring around the wing pouch (arrowhead), and two spots in the notal region. (C) *wg* expression in a leg disc. In leg discs, *wg* is expressed in a ventral wedge. (D) *wg* expression in the genital disc. The two genital discs are fused at their midline. *wg* is expressed in the medial region where the discs are fused. In the following panels, diagrams of the imaginal discs are shown, with the position of the anterior–posterior (A/P) compartment boundary indicated by a double line. (E–H) Characteristic pattern deletions observed in pharate *wg* adults (*wg<sup>CX3</sup>/wg<sup>IG22</sup>*). Regions most frequently deleted in defective discs are shaded onto the regions of the disc that normally give rise to those structures. In most defective eye discs, only the palpus and a patch of postorbital bristles and associated ommatidia are identifiable, although additional trichomed cuticle with no bristles or other landmarks are present, which may represent cuticle from the back of the head. In less defective eye–antennal discs, the entire antennae are deleted except for a patch of trichomed cuticle that we believe, from its position and morphology, corresponds to the dorsal cuticle of the first antennal segment. In the typical wing disc, the wing blade is deleted and only a duplicated notum remains. In the legs, the ventral region of the pattern is deleted and replaced by a mirror-image duplication of the dorsal leg. Generally, the plane of duplication extends through the distal tip of the leg but can

lie more ventrally, in which case it results in distal bifurcations. The genital discs in mutant individuals lack medial structures (penis, hypandrium, spermatheca, vaginal opening) and the vaginal and male lateral plates and claspers are fused along the ventral mid-line. Anal plates and eighth tergites are normal. (I–L) Characteristic pattern deletions observed in pharate *arm* adults partially rescued with *arm* transformants (*arm<sup>XM19</sup>/Y*, BCD7). The spectrum of pattern defects is very similar to that found in *wg* individuals. (M–P) Defects and clones in irradiated *arm* heterozygotes. The positions of clones is based on bristle markers (*y f*) and thus the actual surviving clone may extend into adjacent cuticle which lacks bristles. In the eye disc, clones were restricted to the thorn bristles on the back of the antenna. The highest frequency of defects were observed in the ocellar–occipital region, but in some cases were as extensive as those depicted for the *wingless* homozygotes (E). Note: Position of the anterior–posterior (A/P) compartment boundaries of different discs were determined by the expression pattern of *engrailed* (Brower, 1986) and the fate maps of the discs from transplantation studies. For the antenna, the A/P border is drawn to cut through the row of thorn bristles, which judging from homeotic transformations (Morata and Lawrence, 1979) occupies the dorsal side of the antenna, and the group of larger bristles on the front on the antenna. The A/P boundary location was a bit problematic in this disc, because of differences between conclusions drawn from the fate map and from *en* expression. Structures in our schematic diagrams have been rotated slightly relative to their locations in Haynie and Bryant’s fate map (1988) to make them more consistent with *engrailed* staining; if *en* staining marks the actual compartment boundary, it may differ slightly from that depicted here. It is not known whether the genital disc possesses an A/P boundary so none is shown.

different regions of the segment are differentially sensitive to a reduction in *arm* levels (Wieschaus and Riggleman, 1987). To test for regional specificities during imaginal disc development, we produced clones homozygous for weaker *arm* alleles, assuming that a small but limiting amount of residual *arm<sup>+</sup>* activity might distinguish subtle differences in *arm* requirement. Clones homozygous for *arm<sup>XM19</sup>*, *arm<sup>25B</sup>*, or *arm<sup>H86</sup>* (Table 1) survive at much higher frequencies than amorphic *arm* clones, but only in certain regions of particular discs; these regions frequently correspond to areas of low *wg* expression, as described below.

#### *Asymmetry of the requirement for arm in the leg disc*

When clones of weak alleles of *arm* were examined, dramatic differences in the requirement for *arm* were

discovered between different regions of the same imaginal disc. This was particularly striking in the leg disc, a diagram of which is shown in Fig. 3C. Each leg arises from its own disc, an epithelial sac that enlarges during larval development. During pupation, this disc everts to form the leg. The outermost ring of the leg disc forms the most proximal tissue, closest to the body. The more central rings telescope out, with the center forming the most distal tissue, the claw at the end of the leg. Each disc also has dorsal–ventral and anterior–posterior axes, further defining the respective areas of the leg upon eversion.

There is a very strong bias for *arm<sup>XM19</sup>* clones to be recovered in dorsal regions of the leg disc flanking the anterior–posterior compartment boundary (Fig. 3F). There is also a proximal–distal bias. While many *arm<sup>XM19</sup>* clones survive in the more proximal leg

**Table 2.** Relative survival of small *armadillo* clones induced late in larval development

| Genotype  | Head      |             | Thorax    |             | Abdomen   |             |
|-----------|-----------|-------------|-----------|-------------|-----------|-------------|
|           | 1 bristle | ≥2 bristles | 1 bristle | ≥2 bristles | 1 bristle | ≥2 bristles |
| y control | 39        | 26          | 29        | 51          | 34        | 52          |
| XP33      | 33        | 6           | 13        | 9           | 9         | 1           |
| % yield   | 89        | 25          | 45        | 18          | 26        | 2           |

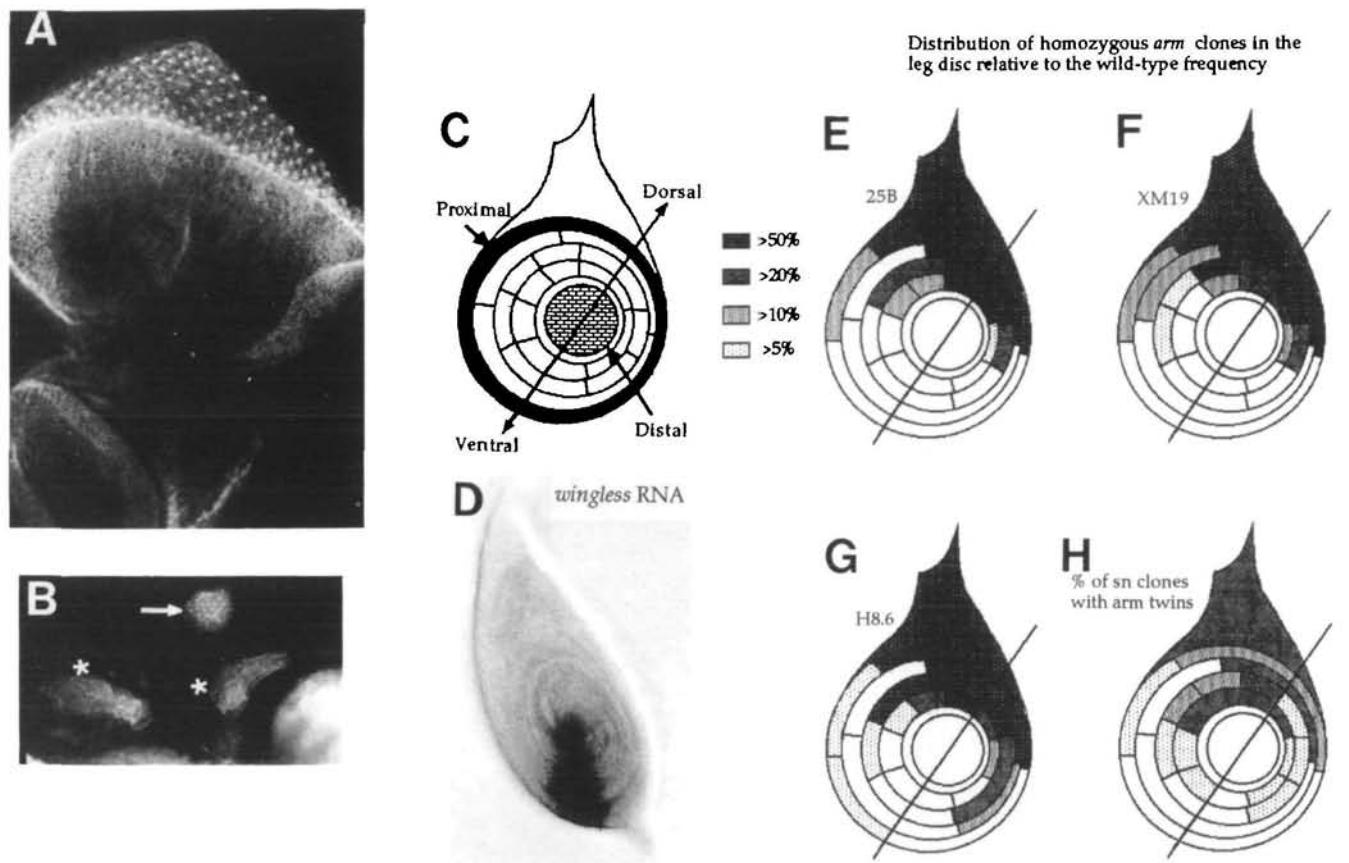


**Fig. 3.** Requirement for *arm* in imaginal discs. (A) Wild-type eye-antennal disc, stained with antibody to *arm* protein. (B) Eye-antennal (arrow) and leg discs (asterisks) from *arm*<sup>H8.6</sup> homozygous larvae, stained with antibody to *arm* protein, at the same magnification as the wild-type disc. Note that, while the eye disc is greatly reduced in size in the mutant, structures resembling clusters of photoreceptors still form. (C) Diagram of a wild-type leg disc, with dorsal and ventral sides labeled and the most proximal and distal tissue indicated by the shaded regions. (D) Expression of *wg* RNA in the leg disc, as in Fig. 2. Expression is limited to a ventral quadrant. (E–G) Survival of homozygous *arm* clones, relative to the survival of the control clones, in different regions of the leg disc. No clones were recovered from unshaded regions. Note that survival is highest in the dorsal region, and lowest in the ventral region which expresses *wg* RNA. (E) *arm*<sup>25B</sup>; (F) *arm*<sup>XM19</sup>; (G) *arm*<sup>H8.6</sup>; (H) percentage of *singed* clones, induced as twin spots with *arm*<sup>XM19</sup>, which have a surviving *arm* twin in the adult cuticle. Only clones induced on the dorsal side have surviving twins, indicating that the biased distribution of *arm* clones is due to differential survival.

segments, none extend into the distal tarsal segments (T2–5) or mark the claw. In contrast, many control clones fill up to half of the leg. A similar dorsal and proximal bias in distribution of leg clones was obtained using *arm*<sup>25B</sup> and *arm*<sup>H8.6</sup> (Fig. 3E, G), arguing that the spatial bias in recovery of clones is a general consequence of reducing *arm* activity. The region of the disc where *arm* clones survive is that farthest from the region that expresses *wg* RNA (Fig. 3D).

While it seemed likely that this bias reflected differential survival, we needed to rule out the possibility that if homozygosity for *arm* shifts ventral clones to more dorsal fates, the clonally derived cells might then migrate to dorsal sites more compatible with their new fate. These two alternate possibilities were previously entertained to explain the behavior of clones in the embryo (Wieschaus and Riggelman, 1987). To evaluate these possibilities, we irradiated individuals *trans*-heterozygous for *arm*<sup>XM19</sup> and the bristle marker

*singed*. Irradiated cells that undergo mitotic recombination produce ‘twin spots’: one daughter cell homozygous for *arm*, the other homozygous for *singed*. The spatial distribution of the *arm*<sup>+</sup> *singed* clones will be random and their position in the adult cuticle will mark where *arm* clones were induced. While *singed* clones marked the four ventral-most bristle rows in the disc with the same frequency that they marked the four dorsal-most rows (130 vs. 123 cases in 278 individuals), only those on the dorsal side of the disc had associated *arm* clones (Fig. 3H). Since each *singed* clone arose with an *arm* twin, *arm* clones on the ventral side must have died; the biased distribution of *arm* clones in the leg is therefore produced by differential survival rather than directed migration.

*Other discs show comparable graded requirements for arm*

Clones homozygous for weak *arm* alleles were re-



covered in the antenna, the notum, the humerus, the proboscis and the analia. We analyzed these clones in a similar though less detailed fashion to the analysis of the leg disc described above. A substantial fraction of the structures derived from the other discs are not covered with bristles, so the distribution of clones could not be determined as accurately as in the legs. In most cases, however, it was possible to determine whether the clones that were detected showed spatial restrictions generally analogous to those in the leg disc. Fig. 2M–P gives a diagrammatic representation of the locations where *arm* clones were recovered in four of the imaginal discs. These diagrams are derived from the fate maps of the different discs, and also indicate the anterior–posterior axis, as determined by the expression of *engrailed* protein (Brower, 1986), and the probable locations of the dorsal and ventral regions, as determined by analysis of homologies between the different discs.

In the leg disc, as described above, *arm* clones were restricted to the dorsal and proximal regions (Fig. 2O, Fig. 3). In most of the other discs examined, clones were also spatially restricted, and arose in regions of those discs that may be homologous to the dorsal, proximal region of the leg. Clones in the eye–antennal disc were restricted to a row of thorn-like bristles on the back of the second antennal segment (Fig. 2M). Cell lineage analysis and examination of the transformations caused by various homeotic mutations (Morata and Lawrence, 1979) suggest that this row is homologous to the dorsal and proximal region of the leg disc where *arm* clones exhibit maximal survival. In wing disc derivatives, all clones were restricted to dorsal part of the anterior compartment, in the region around the notopleural bristles (Fig. 2N). Cell lineage studies (Wieschaus and Gehring, 1976) suggest that this area is clonally related to the region of the leg disc where we detected the highest frequencies of clones. In the proboscis, clones were recovered flanking the anterior–posterior boundary in the prementum, which is derived from the dorsal, most proximal region of the labial disc (Struhl, 1981). No clones were detected in the labellum, a structure ventral to the prementum which, from the transformations observed in various homeotic mutants, is thought to be homologous to the ventral region of the leg (Struhl, 1981). Clones were detected in all bristled regions of the small humerus. Although this structure lacks any apparent proximal–distal organization, the recovered *arm* clones may be derived from the dorsal region of the humeral disc, since the humeral disc also gives rise to a ventral spiracle and associated pleura. The genital disc gives rise to the structures of the analia and genitalia. All clones detected in the genital disc derivatives were found in the ventral anal plates, which occupy a mid-lateral position in the dorsal epithelium of the disc (Fig. 2P).

When the regions where *arm* clones survive (Fig. 2M–P) are compared to the expression pattern of *wg* in each disc (Fig. 2A–D), a striking rule is maintained. Clones with reduced levels of *arm* survive only in regions of the disc that are distant from those

regions that show high levels of *wg* RNA. Conversely, the cells most sensitive to reductions in *arm* activity are those that express *wg* themselves or are adjacent to cells expressing *wg*. The only possible exception is in the wing disc, where the *wg* expression pattern is very complex.

#### *wingless-like phenotypes are produced by arm clone induction or by marginal reductions of arm activity*

Manipulation of *arm* dosage can result in phenotypes similar to those of weak *wg* mutations. Many *arm* heterozygotes that had been irradiated as young larvae showed unusual pattern deletions or duplications as adults, which resemble defects seen in weak *wg* mutants (Fig. 4B, F, and J). These defects were found even in animals carrying strong *arm* alleles, for which few or no clones were found. The defect frequency was similar to the frequency of clones in the *arm*<sup>+</sup> controls. In the eye–antennal disc, defect frequencies were 24% and 20% for *arm*<sup>XK22</sup> and *arm*<sup>XP33</sup>, respectively, compared to a control clone frequency of 31%; in the legs, the defect frequencies were 7% and 5%, compared to a clone frequency of 10%. Defects were not found at significant frequencies in unirradiated *arm* heterozygotes, in irradiated wild-type controls, or in our earlier experiments involving induction of clones homozygous for cell lethals (e.g., *Notch*, *bazooka*, Wieschaus and Noell, 1986). This suggests that pattern deletions are somehow associated with induction of *arm* clones in the disc. In contrast to the random distribution of the *yf* control clones, pattern defects were observed only in defined regions of each disc, suggesting that they may not arise simply from the death or elimination of all homozygous *arm* clones.

To rule out the possibility that these disc defects reflect radiation damage or some peculiarity of clonal analysis, we used a second approach to produce adults with reduced *arm* levels. These flies were obtained using a transformant line (BCD7) carrying the wild-type *arm* gene. Although most transformant lines made using this construct rescue *arm* individuals to full adult viability (Riggleman *et al.* 1989), BCD7 fully rescues only the weakest *arm* alleles, presumably due to a position effect on *arm* expression. Flies carrying a strong allele of *arm* (*arm*<sup>YD35</sup>) and a single copy of the BCD7 transposon die as early pupae. The BCD7 transposon allows flies carrying moderate alleles of *arm* (e.g. *arm*<sup>XM19</sup>) to survive to late pupal development, or to emerge from their pupal cases as adults with a high frequency of imaginal disc defects (Fig. 4D, H, and L).

The imaginal disc defects produced either by clone induction or by use of the *arm* transposon are remarkably similar to each other, and to the defects seen in animals mutant for weak alleles of *wg*, like *wg*<sup>I</sup> or *wg*<sup>CX3</sup> (Fig. 4B, F, and J). In the eye–antennal disc, pattern defects were most often found in the dorsal–medial region of the head (Fig. 4B, C, and D), though in the most severe cases they can result in loss of most of the head capsule (Fig. 4D). A similar medial bias was observed for deletions in the genital disc, resulting in left and right fusions of the vaginal plates (data not

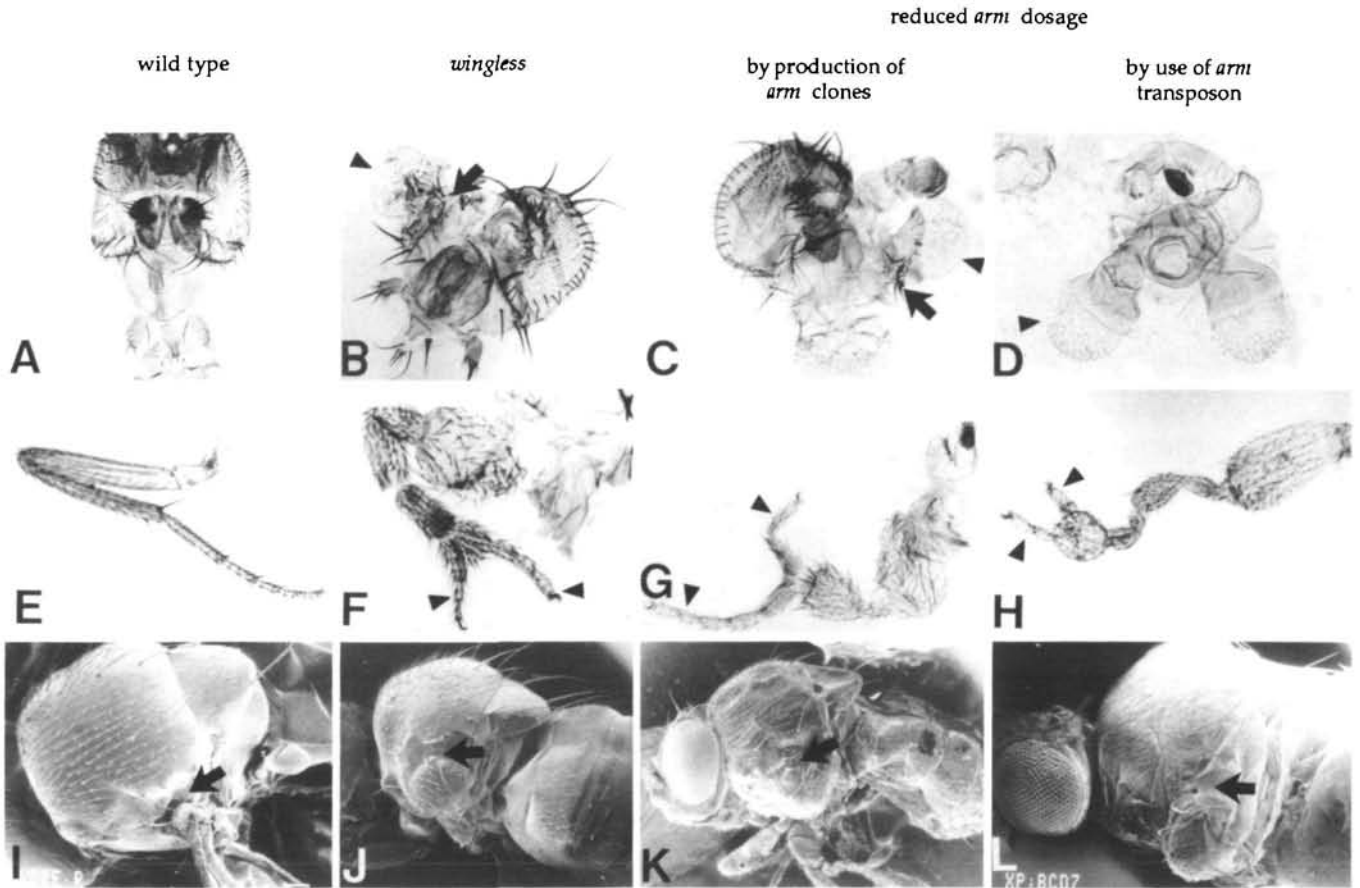


**Fig. 4.** Reduction of *armadillo* expression can phenocopy *wingless*. The figure displays heads (A–D), legs (E–H), and notal tissue (I–L) from wild-type (A, E, and I), *wg* (B, F (both *wg<sup>CX3</sup>/wg<sup>G22</sup>*), and J (*wg<sup>I</sup>/wg<sup>L114</sup>*)), flies from the *arm* clonal analysis experiment (C (*arm<sup>YD35</sup>*), G (*arm<sup>XK22</sup>*), and K (*arm<sup>YD35</sup>*)), and flies carrying a mutation in *arm* and the weakly rescuing *arm* transposon BCD7 (D, H (both *arm<sup>XM19</sup>*), and L (*arm<sup>XP33</sup>*)). In each case, the animals with a *wg* mutation are phenotypically similar to those with reduced *arm* dosage. Heads (compare A with B–D) show varying degrees of reduction in the head capsule (arrow), while eye tissue remains (arrowhead). In the most extreme cases (e.g. D), there is little left except reduced eyes (arrowhead). Legs (compare E with F–H) show deletions of ventral tissue and duplications of dorsal tissue, sometimes resulting in distal branching (arrowheads). In the notal region (compare I with J–L), the distal wing blade is lost, and replaced by a duplicated notum. The joint between wing and notum in the wild-type animal, and the plane of the mirror-image duplication in the mutant animals are indicated by arrows.

shown). In leg and wing disc derivatives, pattern deletions were frequently associated with a mirror-image duplication of the remaining elements. Because all the surviving cells are *arm<sup>+</sup>*, the duplications observed in the *arm* clonal experiments are ‘non-autonomous’ consequences. In the legs, most defects involve ventral and distal deletions, with duplications of dorsal structures (Fig. 4F, G, and H), while in the wing disc, the distal wing blade is deleted, and replaced by more proximal and dorsal notal tissue (Fig. 4J, K, and L). The pattern elements deleted in most of these discs are formed at or near regions that express high levels of *wg* RNA (Compare with Fig. 2). The correspondence between the pattern deletions, the regions that require high levels of *arm* activity, and the local expression patterns of *wg* suggests that the *wg*-like defects may reflect a cellular role for *arm* in the reception or interpretation of the *wg* signal.

#### *Accumulation of arm protein in larval tissues*

To determine the pattern of *arm* protein accumulation in discs, we used an antibody to *arm* (Riggleman *et al.* 1990) to stain larvae. *arm* protein is expressed in a variety of larval tissues, but its levels in the different tissues vary greatly. There is little or no *arm* protein in muscle, there is more in salivary glands, and there are very high levels in imaginal discs (Fig. 5B and data not shown). In embryos *arm* and actin often co-localize (Riggleman *et al.* 1990), but the correlation between relative levels of *arm* and actin in different larval tissues was poor (Fig. 5B vs. 5C). The elevated levels of *arm* protein in imaginal discs are consistent with the results with *arm<sup>H86</sup>* mentioned above, where discs appear to require more *arm* than other larval tissues. We also noted that, in all of the discs, the accumulation of *arm* protein is highly polarized within cells. Each disc is an epithelial sac, with the apical side of the cells on the

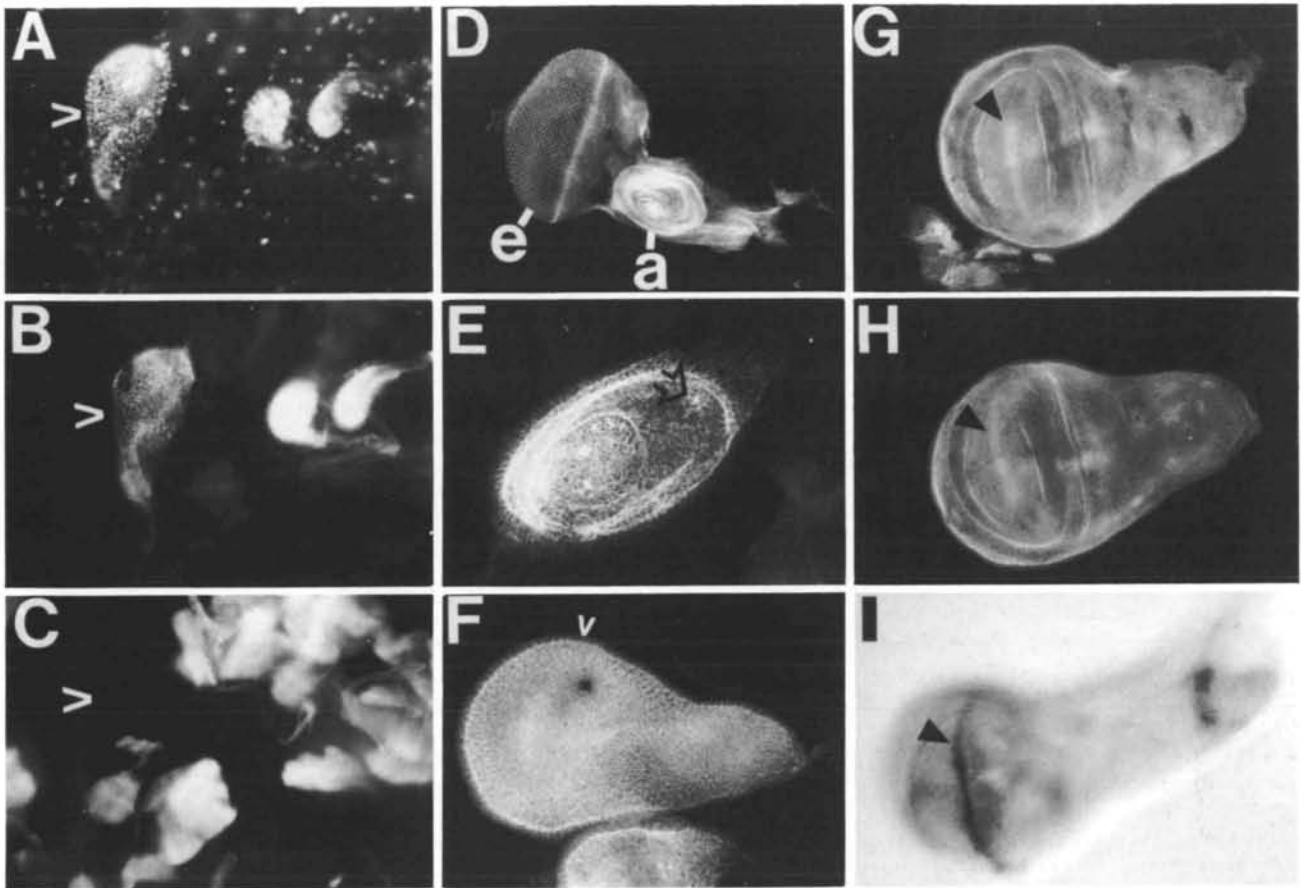


**Fig. 5.** Expression of *arm* protein in imaginal tissues. (A–C) Comparison of the staining patterns obtained using Hoechst (A), which stains all nuclei, antiserum to *armi* protein (B), or phalloidin (C), which labels accumulations of F-actin. In this field, one can see a wing imaginal disc (indicated by an arrowhead) and two leg imaginal discs, surrounded by muscle and other tissues. Actin is expressed very strongly in muscle tissue, but much more weakly in the imaginal discs (C). *arm*, in contrast, is highly enriched in imaginal discs relative to muscle or other tissues (B). (D–H) *arm* protein accumulation in the eye–antennal disc (D; e=eye disc and a=antennal disc), leg disc (E), and young (F) and older (G and H) wing imaginal discs. Expression of *arm* in the eye disc is described in more detail in Peifer and Wieschaus (1990b). In the leg disc, there is heavy accumulation in a reproducible pattern of dots, one of which is indicated by an arrow in E. The polarized accumulation of *arm* in disc cells can be seen in the edge-on view indicated in F by an arrow. Note that in wing discs (F–H), there often appears to be a stripe of increased *arm* protein accumulation across the wing blade (indicated by the arrowhead in G and H), which is similar in location to the stripe of *wg* RNA expression seen in the wing disc (arrowhead in I).

inside. *arm* protein accumulates heavily on the apical surface, less heavily on the lateral sides where cells contact one another, and little is found on the basal surface (e.g. Fig. 5F). Polarized accumulation is also a feature of *arm* expression in a number of other cell types (Riggleman *et al.* 1990; Peifer and Wieschaus, 1990b). We have recently noted that *arm* is the *Drosophila* homolog of the mammalian junctional protein plakoglobin. Many features of *arm* protein accumulation in imaginal discs, such as cell surface localization, polarized accumulation, and co-localization with actin in some situations and not others, are features shared with plakoglobin (e.g. Cowin *et al.* 1986).

In embryos, *arm* protein is present throughout each segment, but accumulates to higher levels in cells that express *wg* (Riggleman *et al.* 1990). We evaluated whether there are similar regional differences in *arm*

accumulation within each imaginal disc, and whether they correlate with *wg* expression. However, unlike the early embryonic epidermis, which is a relatively smooth sheet of similarly sized cells, the epithelium of the imaginal disc is composed of both small and large cells, and it is folded in a complex manner. Since *arm* is localized to the inner surface of the membrane, these differences in cell size and the folding result in apparent differences in *arm* accumulation, which may simply reflect differences in the amount of membrane in different regions. In addition, as the disc grows, these features change rapidly. While at any given moment, there are apparent patterns of *arm* accumulation (Fig. 5), we were unable to correlate most of the regional differences in *arm* accumulation that we observed with *wg* expression. We did, however, observe one consistent correlation between *wg* expression and *arm* accumulation in the wing disc. *wg*

expression in the wing disc is complex (Figs 2B and 5I), but includes a stripe across the developing wing margin. There is a faint but consistent stripe of *arm* protein accumulation in this same position (compare Fig. 5F, G, H, and I).

## Discussion

We have examined the role of the *armadillo* (*arm*) gene in pattern formation in imaginal discs, the precursors of the adult cuticle. *arm* is a segment polarity gene, required for pattern formation within each embryonic segment. In particular, it is a member of the *wingless*-class of segment polarity genes, which all share a similar embryonic phenotype. We have established that mutations in *arm* and *wingless* (*wg*) are indistinguishable in their embryonic consequences, and that they also seem to have very similar consequences on imaginal disc development. These similarities strongly suggest that some of the members of the *wg*-class of segment polarity genes encode different components of a common molecular pathway required for proper pattern formation during both the embryonic and the adult stages.

### *arm* is required for imaginal disc development

Embryonic patterning in *Drosophila* occurs in two phases, which differ in their cellular environments. After fertilization thirteen rounds of nuclear division occur without cell division, producing a syncytial blastoderm – one large ‘cell’ with six thousand nuclei. At this point all of the nuclei simultaneously cellularize. As a result, zygotic genes acting early in pattern formation, the gap and pair-rule genes, respond to the positional information set up by maternal genes within the syncytium, without cell membrane boundaries. These zygotic genes encode transcription factors which rely on the preimposed maternal pattern or interact with each other within the syncytium. By the cellular blastoderm stage, these genes subdivide the embryo into what will become the segments, and activate the next set of genes in the hierarchy, the segment polarity genes.

The products of the segment polarity genes operate in a new environment, a sheet of epithelial cells. As a consequence, cell–cell interactions now assume a prominent role, influencing the regulation of segment polarity genes and their subsequent determination of pattern within the segment. Many segment polarity genes encode proteins with probable roles in intercellular communication. For example, *wg* encodes a secreted factor, which may serve as a signaling molecule (van den Heuvel *et al.* 1989), *patched* encodes a transmembrane protein (Hooper and Scott, 1989; Nakano *et al.* 1989), and *fused* encodes a Ser/Thr kinase (Preat *et al.* 1990). Different classes of segment polarity genes, like the *wg*-class or the *patched*-class, are required in different cells within each embryonic segment. It is possible that these different classes each define separate or interacting biochemical pathways

mediating intercellular communication within segments.

The segment polarity genes also differ from the gap and pair-rule genes in their later roles in pattern formation. While some gap and pair-rule genes function in the embryonic nervous system, most are not required after embryogenesis. In contrast, many segment polarity genes do play roles during later development. In general, these roles were discovered because of the existence of weak or unusual alleles of certain segment polarity genes; flies mutant for these alleles survive embryogenesis, but emerge as adults with specific pattern defects (e.g. Sharma and Chopra, 1976; Kornberg, 1981; Phillips *et al.* 1990). These later roles for segment polarity genes may reflect the fact that pattern formation in the imaginal discs, which give rise to the adult cuticle, occurs in an epithelial sheet, like the later stages of embryonic pattern formation. Genes that are required for cell–cell communication, like the segment polarity genes, may be required for both processes.

No adult viable alleles of the segment polarity gene *arm* exist. Thus, we have assessed the role of *arm* in imaginal disc development by examining the consequences of a pupal lethal allele, by creating clones of *arm* mutant tissue in otherwise wild-type flies, and by artificially manipulating the levels of *arm* using transgenic flies. In these ways, we have demonstrated that, like many other segment polarity genes, *arm* has an important role in imaginal disc development.

There are both similarities and differences between the role of *arm* in embryonic and adult patterning. One apparent difference is that strong *arm* alleles cause transformations in the embryo (Wieschaus and Riggleman, 1987), but clones homozygous for the same alleles die in imaginal discs. This difference may only reflect the fact that maternal *arm* product is provided to the egg in quantities sufficient to partially rescue the effect of *arm* mutations on the embryonic pattern (Wieschaus and Noell, 1986). Induction of an amorphic *arm* clone during cellular blastoderm will only reduce the level of *arm* product in those cells down to the level provided by maternal perdurance. In contrast, due to the extensive proliferation and growth of the larval clones between induction and disc differentiation, any maternal or zygotic product produced before clone induction is subsequently diluted out by growth. This may increase the severity of the loss of *arm* in discs relative to its loss in embryos.

One similarity between the behavior of *arm* in embryos and imaginal discs is that, in both, *arm* alleles form the same allelic series. The stronger the embryonic phenotype of an *arm* mutation (Peifer and Wieschaus, 1990b), the stronger is its effects on imaginal discs (Table 1). While there are a few apparent anomalies in this comparison, these may be due in part to statistical fluctuations when counting small numbers of clones. Another striking similarity between *arm* action in embryos (Wieschaus and Riggleman, 1987) and imaginal discs (these results) is that, in both, *arm* acts autonomously, with mutant cells adopting a mutant

destiny regardless of whether they are surrounded by wild-type neighbors. This contrasts with the non-autonomy of *wg*, in which mutant cells can be rescued by their wild-type neighbors (Morata and Lawrence, 1977). The question of autonomy is important in assigning a cellular function to these two genes. The non-autonomy of *wg* is consistent with its proposed role as a secreted signaling molecule. Likewise, the autonomy of *arm* function is consistent with the intracellular localization of *arm* protein (Riggleman *et al.* 1990; Fig. 5) and with the recent determination (Peifer and Wieschaus, 1990b) that *arm* is the *Drosophila* homolog of the mammalian protein plakoglobin, a protein that functions on the interior of the cell as a component of adhesive junctions (Cowin *et al.* 1986).

There are cases where apparently 'non-autonomous' consequences of *arm* mutations are seen. When clones were induced in animals carrying strong *arm* alleles, no clones survived, but there were numerous pattern defects involving wild-type cells. If *arm* acts cell autonomously, how do we explain these effects of mutant cells on wild-type cells? The frequency of defects was close to the frequency of clones in the controls. We therefore suspect that these defects occur in animals in which a clone of *arm* mutant tissue was produced. While the clone died before morphogenesis, its presence earlier in development may have had an influence on its neighbors. It is not uncommon for mutations in genes whose products act autonomously, and thus inside each cell, to have an effect on adjacent cells. For example, in embryos mutant for strong alleles of *engrailed* (*en*), a homeodomain transcription factor, cells outside of the *en*-expressing domain are affected, as assayed both by molecular markers like expression of *wg* RNA (Martinez-Arias *et al.* 1988) or by their final morphology. In both the case of *arm* and of *en*, these consequences are almost certainly results of the cell-cell interactions operating in the epithelial sheet. We have shown above that *arm* is required in embryos for the maintenance of *wg* expression. One obvious possible explanation for the non-autonomous consequences of *arm* clones is that the induction of an *arm* clone may affect the expression pattern of *wg* in that disc, leading to non-autonomous effects on neighboring cells. Similar 'domineering non-autonomy' was seen for clones of the segment polarity gene *hedgehog* (Mohler, 1988).

Both the embryonic ectoderm and the imaginal discs express high levels of *arm*. In both, much of the *arm* protein seems to be localized to the cell surface and, in some cases, this cell surface accumulation is polarized within individual cells. Such polarization, also seen in the ovary and certain embryonic and larval tissues (Riggleman *et al.* 1990; Peifer and Wieschaus, 1990b), is very pronounced in the discs. There is substantial cell surface *arm* on the apical and lateral sides of imaginal disc cells, but little or no accumulation on the basal surface. In the embryonic epidermis, the pattern of *arm* protein accumulation is relatively simple; there is a uniform baseline of expression in all cells, and a *wg*-dependent elevated accumulation in the *wg* domains

(Riggleman *et al.* 1990). It is difficult to compare patterns of *arm* accumulation in the embryo and the discs because of the complexities of disc morphology. Discs are composed of large and small cells in a complex folded epithelium, giving the appearance of patterns of *arm* accumulation which may only reflect differences in density of cell membranes between different regions. We were unable to draw many convincing correlations between *wg* expression and *arm* protein accumulation. One possible correlation is in the wing disc, where the stripe of *wg* RNA along the future wing margin may be echoed by a corresponding increase in *arm* protein accumulation (Fig. 5).

Perhaps the most striking similarity between the embryo and the imaginal discs is that different cells display differing requirements for *arm* activity depending on their position. In the embryo, the cells most sensitive to the loss of *arm* are the cells of the posterior part of the anterior compartment, those cells that form the middle part of the naked cuticle (Wieschaus and Riggleman, 1987; Riggleman, 1989; Peifer and Wieschaus, 1990b). The cells of the denticle belt are least sensitive to *arm* loss. Likewise, in the leg disc, for example, ventral and distal cells are most sensitive to loss, while dorsal and proximal cells are least sensitive (Fig. 3). The other discs seem to show similar graded requirements for *arm* activity.

#### *arm* and *wg* appear to act together in pattern formation

The most interesting aspect of the regional sensitivity to the levels of *arm* in both the embryo and the imaginal discs is the correlation of both with *wg* expression. The regions most sensitive to loss of *arm* are those that normally express *wg* RNA, while the regions farthest from the *wg*-expressing domain are least sensitive to *arm* loss. In the embryo, even the weakest *arm* mutations affect cells of the *wg* domain, transforming naked cuticle to denticle belt. Likewise, in the leg disc one can superimpose the wedge-shaped region of *wg* expression on to the map of the region most sensitive to the loss of *arm* activity.

There are a number of other connections between *wg* and *arm*. Mutations in both loci have indistinguishable effects on embryonic pattern, as assayed by their effect on the cuticle and by the expression patterns of molecular markers such as *en* (Fig. 1). In the embryo, the maintenance of *wg* expression is dependent on *arm* function (Fig. 1), while the *wg* gene is required for the post-transcriptional regulation of *arm* protein (Riggleman *et al.* 1990). Finally, weak mutations in *wg* result in effects on the adult cuticle that are very similar to those produced by either clones of *arm* mutations or by slight reductions in the level of *arm* activity produced using transposons carrying *arm*<sup>+</sup>. Thus, both in the embryo and in the imaginal discs, mutations in *arm* and *wg* are nearly indistinguishable in their consequences.

The segment polarity genes fall into classes according to which region of the embryonic segment is affected. While numerous segment polarity genes have weak alleles that give imaginal disc phenotypes, these



phenotypes are often very different. It is difficult to determine whether the phenotypic differences reflect real differences between the cellular machinery used in pattern formation in embryos and in imaginal discs, or whether they simply reflect differences in allele strength, which hide underlying similarities. The work above on *arm* and *wg*, along with the characterization of two other members of the *wg*-class of segment polarity genes, *dishevelled* and *porcupine* (Klingensmith *et al.* submitted), has demonstrated that at least these four genes are virtually indistinguishable both in embryonic phenotype and also in their effects on imaginal discs.

These similarities suggest two conclusions about pattern formation in imaginal discs. First, they support the idea that *arm*, *wg*, *porcupine*, and *dishevelled* function together in the same cellular pathway, which is believed to involve the production, reception, and interpretation of an intercellular signal encoded by the *wg* gene. The sequence identities between *arm* and the mammalian junctional protein plakoglobin suggest that the signal may be transduced *via* a new pathway involving these junctional complexes (This possibility is discussed more fully in Peifer and Wieschaus, 1990b). Second, the similarities suggest that the mechanisms of pattern formation in embryos and imaginal discs, while seemingly quite different, may in fact utilize the same cellular machinery. A few other components of the embryonic pattern formation machinery have been implicated in imaginal disc patterning. These include both the other segment polarity genes, along with *decapentaplegic*, the homolog of mammalian TGF- $\beta$  (Posakony, 1987). There is suggestive evidence that another pair of segment polarity genes, *en* and *hedgehog*, may function together in both processes, and thus may define another pathway (Mohler, 1988). Our knowledge of patterning in the embryo may help us understand pattern formation in the imaginal discs.

#### Other roles for armadillo

While much of the phenotype of *arm* in the embryo and imaginal discs can be explained by its probable involvement in the reception of the *wg* signal (either directly or indirectly), *arm* may also play additional roles. Clones of strong alleles of *arm* are not viable, regardless of where in the disc they are found. Likewise, the process of dorsal closure in the embryo is interrupted in strong *arm* mutants but not by mutations in *wingless*. *arm* is also expressed highly in tissues like the eye disc and the salivary glands, which seem neither to express nor to require *wg*. The mammalian *arm* homolog, plakoglobin, is found in a very wide variety of cell junctions in numerous cell types (e.g. Cowin *et al.* 1986). It seems probable that these different junctions may serve a number of different cellular functions, some of them required for *wg* or perhaps other signal transduction pathways, and some serving purely adhesive functions. The other phenotypes of *arm* mutations may uncover some of these additional functions.

We thank Nick Baker, Bob Holmgren, John Klingensmith, Alfonso Martinez-Arias, Roel Nusse, Norbert Perrimon,

Roger Phillips, Marcel van den Huevel, and Robert Whittle for sharing data prior to publication. Nipam Patel kindly provided antibody, and Chihiro Hama and Thomas Kornberg provided the *en*- $\beta$ -galactosidase stock, before publication. We are also grateful to Beth Bucher, Iva Greenwald, Carol Ann McCormick, Marya Postner, and Lesilee Simpson for careful reading and very helpful suggestions on the manuscript, and to members of the Wieschaus and Schüpbach laboratories for many helpful discussions. The experiments were supported by a National Institute of Health Research Grant to E. W., an NIH postdoctoral fellowship to M.P., and an NIH training grant (C.R., B.R.).

#### References

- BAKER, N. E. (1987). Molecular cloning of sequences from *wingless*, a segment polarity gene in *Drosophila*: the spatial distribution of a transcript in embryos. *EMBO J.* **6**, 1765–1773.
- BAKER, N. E. (1988a). Embryonic and imaginal requirements for *wg*, a segment polarity gene in *Drosophila*. *Devl Biol.* **125**, 96–108.
- BAKER, N. E. (1988b). Transcription of the segment polarity gene *wingless* in the imaginal discs of *Drosophila*, and the phenotype of a pupal-lethal *wg* mutation. *Development* **102**, 489–497.
- BROWER, D. (1986). *engrailed* gene expression in *Drosophila* imaginal discs. *EMBO J.* **5**, 2649–2656.
- CABRERA, C. V., ALONSO, M. C., JOHNSTON, P., PHILLIPS, R. G. AND LAWRENCE, P. A. (1988). Phenocopies induced with antisense RNA identify the *wingless* gene. *Cell* **50**, 567–576.
- CARROLL, S. B. AND WHITE, J. S. (1989). The role of the *hairy* gene during *Drosophila* morphogenesis: stripes in imaginal discs. *Genes Dev.* **3**, 905–916.
- COWIN, P., KAPPELL, H.-P., FRANKE, W. W., TAMKUN, J. AND HYNES, R. O. (1986). Plakoglobin: A protein common to different kinds of intercellular junctions. *Cell* **46**, 1063–1073.
- DI NARDO, S., KUNER, J. M., THEIS, J. AND O'FARRELL, P. H. (1985). Development of the embryonic pattern in *D. melanogaster* as revealed by the accumulation of the nuclear *engrailed* protein. *Cell* **43**, 59–69.
- DI NARDO, S., SHER, E., HEEMSKERK-JONGENS, J., KASSIS, J. A. AND O'FARRELL, P. H. (1988). Two-tiered regulation of spatially patterned *engrailed* gene expression during *Drosophila* embryogenesis. *Nature* **322**, 604–609.
- GERGEN, J. P. AND WIESCHAUS, E. F. (1986). Localized requirements for gene activity in segmentation of *Drosophila* embryos: Analysis of *armadillo*, *fused*, *giant* and *unpaired* mutations in genetic mosaics. *Roux' Arch. devl Biol.* **195**, 49–62.
- HAMA, C., ALI, Z. AND KORNBERG, T. B. (1990). Region specific recombination and expression are directed by portions of the *Drosophila* *engrailed* promoter. *Genes Dev.* **4**, 1079–1093.
- HAYNIE, J. L. AND BRYANT, P. J. (1986). Development of the eye-antenna imaginal disc and morphogenesis of the adult head in *Drosophila melanogaster*. *J. exp. Zool.* **237**, 293–308.
- HOOPER, J. E. AND SCOTT, M. P. (1989). The *Drosophila* *patched* gene encodes a putative membrane protein required for segmental patterning. *Cell* **59**, 751–765.
- INGHAM, P. (1988). The molecular genetics of embryonic pattern formation in *Drosophila*. *Nature* **335**, 25–34.
- KLINGENSMITH, J., NOLL, E. AND PERRIMON, N. (1989). The segment polarity phenotype of *Drosophila* involves differential tendencies toward transformation and cell death. *Devl Biol.* **134**, 130–145.
- KLINGENSMITH, J., VAN DEN HEUVEL, M., ZACHARY, K., NUSSE, R. AND PERRIMON, N. *porcupine* and *dishevelled* function in the signalling pathway of *wingless*, the *Drosophila* *wnt-1* homolog. submitted.
- KORNBERG, T. (1981). *engrailed*: A gene controlling compartment and segment formation in *Drosophila*. *Proc. natn. Acad. Sci. U.S.A.* **78**, 1095–1099.
- LINDSLEY, D. L. AND GRELL, E. L. (1968). Genetic variations of *Drosophila melanogaster*. *Carnegie Inst. Wash. Publ.* **627**.



- LINDSLEY, D. L. AND ZIMM, G. (1986). The genome of *Drosophila melanogaster* Part 2: lethals; maps. *Dros. Inform. Serv.* **64**.
- MARTINEZ-ARIAS, A., BAKER, N. AND INGHAM, P. (1988). Role of the segment polarity genes in the definition and maintenance of cell states in the *Drosophila* embryo. *Development* **103**, 157–170.
- MOHLER, J. (1988). Requirements for *hedgehog*, a segment polarity gene, in patterning larval and adult cuticle of *Drosophila*. *Genetics* **120**, 1061–1072.
- MORATA, G. AND LAWRENCE, P. A. (1977). The development of *wingless*, a homeotic mutant of *Drosophila*. *Devl Biol.* **56**, 227–240.
- MORATA, G. AND LAWRENCE, P. A. (1979). Development of the eye-antenna imaginal disc of *Drosophila*. *Devl Biol.* **70**, 355–371.
- NAKANO, Y. I., GUERRERO, I., HILDAGO, A., TAYLOR, A., WHITTLE, J. AND INGHAM, P. (1989). A protein with several possible membrane spanning domains encoded by the *Drosophila* segment polarity gene *patched*. *Nature* **341**, 508–513.
- NÜSSLEIN-VOLHARD, C., WIESCHAUS, E. AND KLUDING, H. (1984). Mutations affecting the pattern of the larval cuticle in *Drosophila melanogaster*. I. Zygotic loci on the second chromosome. *Wilhelm Roux' Arch. devl Biol.* **193**, 267–282.
- NÜSSLEIN-VOLHARD, C. AND WIESCHAUS, E. (1980). Mutations affecting segment number and polarity in *Drosophila*. *Nature* **287**, 795–801.
- PATEL, N., MARTIN-BLANCO, E., COLEMAN, K. G., POOLE, S. J., ELLIS, M. C., KORNBURG, T. B. AND GOODMAN, C. S. (1989). Expression of *engrailed* proteins in arthropods, annelids and chordates. *Cell* **58**, 955–968.
- PEIFER, M. AND WIESCHAUS, E. (1990a). Mutations in the *Drosophila* gene *extradenticle* affect the way specific homeodomain proteins regulate segmental identity. *Genes Dev.* **4**, 1209–1223.
- PEIFER, M. AND WIESCHAUS, E. (1990b). The segment polarity gene *armadillo* encodes a functionally modular protein that is the *Drosophila* homolog of human plakoglobin. *Cell* **63**, 1167–1178.
- PERRIMON, N., ENGSTROM, L. AND MAHOWALD, A. P. (1989). Zygotic lethals with specific maternal effect phenotypes in *Drosophila melanogaster*. I. Loci on the X chromosome. *Genetics* **121**, 333–352.
- PERRIMON, N. AND MAHOWALD, A. P. (1987). Multiple functions of segment polarity genes in *Drosophila*. *Devl Biol.* **119**, 587–600.
- PHILLIPS, R. G., ROBERTS, I. J. H., INGHAM, P. W. AND WHITTLE, J. R. S. (1990). The *Drosophila* segment polarity gene *patched* is involved in a position-signaling mechanism in imaginal discs. *Development* **110**, 105–114.
- POSAKONY, L. (1987). The role of the DPP-C in the development of the imaginal discs in *Drosophila melanogaster*. Ph.D. dissertation, Harvard University, Cambridge.
- PREAT, T., THEROND, P., LAMOUR-ISNARD, C., LIMBOURG-BOUCHON, B., TRICARE, H., ERK, I., MARIOL, M.-C. AND BUSSON, D. (1990). A putative serine/threonine kinase encoded by the segment polarity *fused* gene of *Drosophila*. *Nature* **347**, 87–89.
- RIGGLEMAN, B. (1989). Molecular and genetic analysis of the *armadillo* locus of *Drosophila melanogaster*. Ph.D dissertation, Princeton University, Princeton.
- RIGGLEMAN, B., SCHEDL, P. AND WIESCHAUS, E. (1990). Spatial expression of the *Drosophila* segment polarity gene *armadillo* is post-transcriptionally regulated by *wingless*. *Cell* **63**, 549–560.
- RIGGLEMAN, B., WIESCHAUS, E. AND SCHEDL, P. (1989). Molecular analysis of the *armadillo* locus: uniformly distributed transcripts and a protein with novel internal repeats are associated with a *Drosophila* segment polarity gene. *Genes Dev.* **3**, 96–113.
- RUISEWIJK, F., SCHUERMANN, M., WAGENAAR, E., PARREN, P., WEIGEL, D. AND NUSSE, R. (1987). The *Drosophila* homologue of the mouse mammary oncogene *int-1* is identical to the segment polarity gene *wingless*. *Cell* **50**, 647–657.
- SHARMA, R. P. AND CHOPRA, V. L. (1976). Effects of the *wingless* (*wg*<sup>1</sup>) mutation on wing and haltere development in *Drosophila melanogaster*. *Devl Biol.* **48**, 461–465.
- SIMPSON, L. AND WIESCHAUS, E. (1990). Zygotic activity of the *nullo* locus is required to stabilize the actin-myosin network during cellularization in *Drosophila*. *Development* **110**, 851–863.
- STRUHL, G. (1981). Anterior and posterior compartments in the proboscis of *Drosophila*. *Devl Biol.* **84**, 372–385.
- STRUHL, G. (1989). Differing strategies for organizing anterior and posterior body pattern in *Drosophila* embryos. *Nature* **338**, 741–744.
- TAUTZ, D. AND PFEIFLE, C. (1989). A non-radioactive *in situ* hybridization method for the localization of specific RNAs in *Drosophila* embryos reveals translational control of the segmentation gene *hunchback*. *Chromosoma* **98**, 81–85.
- VAN DEN HEUVEL, M., NUSSE, R., JOHNSTON, P. AND LAWRENCE, P. A. (1989). Distribution of the *wingless* gene product in *Drosophila* embryos: a protein involved in cell-cell communication. *Cell* **59**, 739–749.
- WIESCHAUS, E. AND GEHRING, W. (1976). Clonal analysis of primordial disc cells in the early embryo of *Drosophila melanogaster*. *Devl Biol.* **50**, 249–263.
- WIESCHAUS, E. AND NOELL, E. F. (1986). Specificity of embryonic lethal mutations in *Drosophila* analysed in germ line clones. *Roux' Arch. devl Biol.* **195**, 63–73.
- WIESCHAUS, E. AND NÜSSLEIN-VOLHARD, C. (1986). Looking at embryos. In *Drosophila, A Practical Approach* (D. B. Roberts, ed.), IRL Press, Oxford, England.
- WIESCHAUS, E., NÜSSLEIN-VOLHARD, C. AND JÜRGENS, G. (1984). Mutations affecting the pattern of the larval cuticle in *Drosophila melanogaster*. III. Zygotic loci on the X-chromosome and fourth chromosome. *Wilhelm Roux' Arch. devl Biol.* **193**, 296–307.
- WIESCHAUS, E. AND RIGGLEMAN, R. (1987). Autonomous requirements for the segment polarity gene *armadillo* during *Drosophila* embryogenesis. *Cell* **49**, 177–184.
- ZUSMAN, S. D., COULTER, D. AND GERGEN, J. P. (1985). Lethal mutations induced in the proximal X-chromosome of *Drosophila melanogaster* using P-M hybrid dysgenesis. *Dros. Inf. Serv.* **61**, 217–218.

(Accepted 20 December 1990)